Electronic Supplementary Material (ESI) for Journal of Materials Chemistry C.
This journal is © The Royal Society of Chemistry 2018

Integrated Strength and Toughness in Calcium Alginate/Graphene Film for Highly Efficient Electromagnetic Interference Shielding

Li-Chuan Jia,[a] Wen-Jin Sun,[a] Chang-Ge Zhou,[a] Ding-Xiang Yan,*[b] Quan-Chao Zhang,[c] and Zhong-Ming Li*[a]

[a]College of Polymer Science and Engineering, State Key Laboratory of Polymer Materials Engineering, Sichuan University, Chengdu, 610065, China.

[b]School of Aeronautics and Astronautics, Sichuan University, Chengdu 610065, China

[c]School of Materials Science and Engineering, East China Jiaotong University, Nanchang 330013, China

*E-mail addresses: yandingxiang@scu.edu.cn (D-X Yan), zmli@scu.edu.cn (Z-M Li)

1. The power coefficient including reflection coefficient (R), absorption coefficient (A), and transmission coefficient (T) as well as EMI SE (SE_{total}), microwave reflection (SE_R) and microwave absorption (SE_A) from scattering parameters

The R, T, and A can be obtained by using measured scattering parameters, as given below:[1]

$$R = |S_{11}|^2 \quad (1)$$

$$T = |S_{21}|^2 \quad (2)$$

$$A = 1 - R - T \quad (3)$$

Then SE_{total}, SE_R, SE_A can be calculated as follows:

$$SE_R = -10\lg(1-R) \quad (4)$$

$$SE_A = -10\lg\left(\frac{T}{1-R}\right) \quad (5)$$

$$SE_{total} = SE_R + SE_A + SE_M \quad (6)$$

where SE_M is the microwave multiple internal reflections, which can be negligible when SE_{total} is higher than10 dB.[1]

2. The schematic diagram for the transformation of sodium alginate (SA) to calcium alginate (CA)

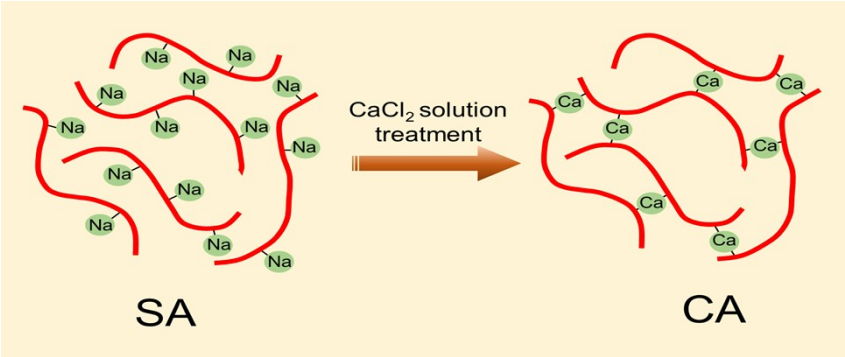

Fig. S1 Schematic diagram for the transformation of SA to CA

3. The energy dispersive spectroscopy (EDS) mapping analysis of the SA， CA and rGO-I films

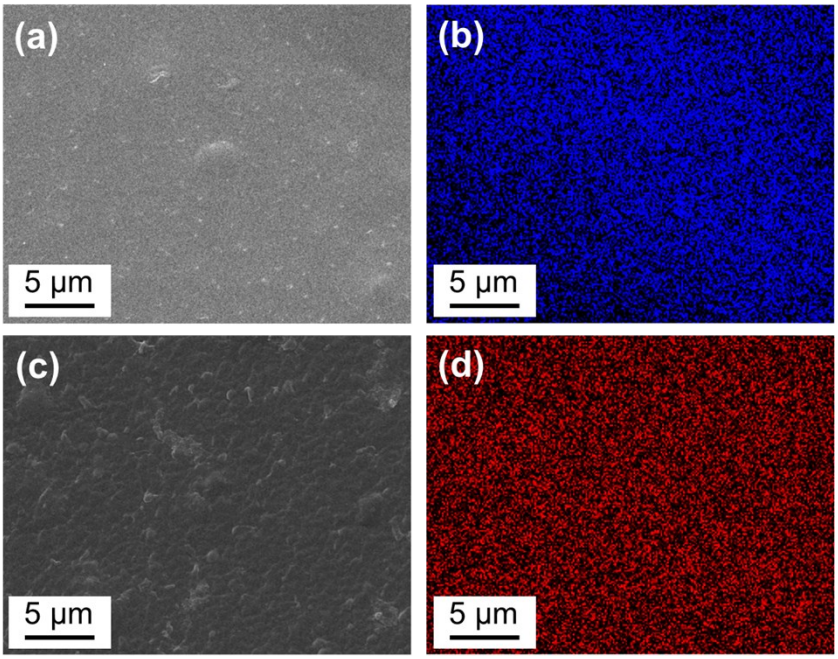

Fig. S2 (a) SEM image of the SA film surface and (b) the corresponding Na element mapping. (c) SEM image of the CA film surface and (d) the corresponding Ca element mapping. The EDS results reveal that a generous amount of Ca element is observed after the SA treated by the $CaCl_2$ solution, indicating the successful transformation of SA to CA.

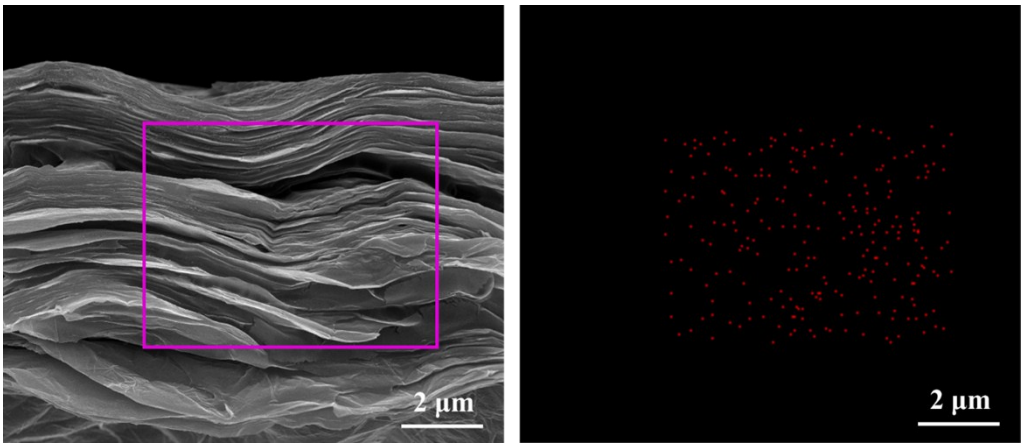

Fig. S3 (a) SEM images of rGO-I film and (b) the corresponding Ca element mapping. The Ca elemental mapping of rGO-I shows that Ca element is still remained after reduction by HI.

4. The Fourier transform infrared (FTIR) spectra of the rGO, rGO-Ca^{+} and rGO/CA films

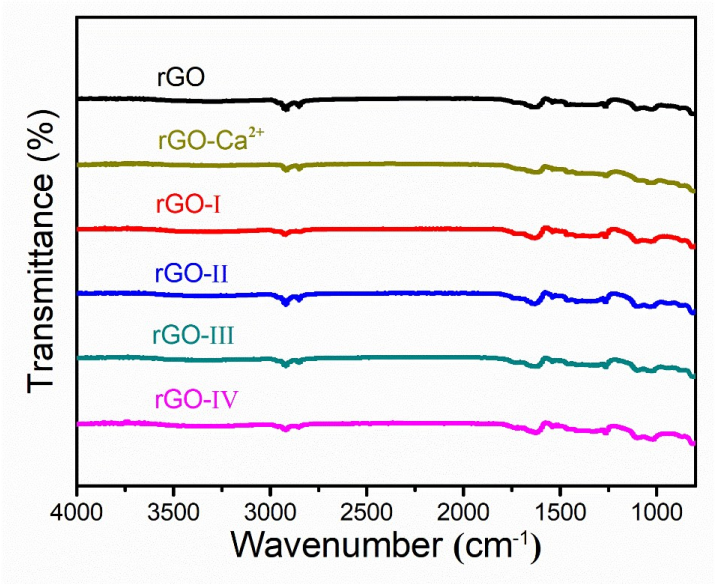

Fig. S4 FTIR spectra of rGO, rGO-Ca^{2+} and rGO/CA films;

5. The power coefficients of the rGO and rGO/CA films

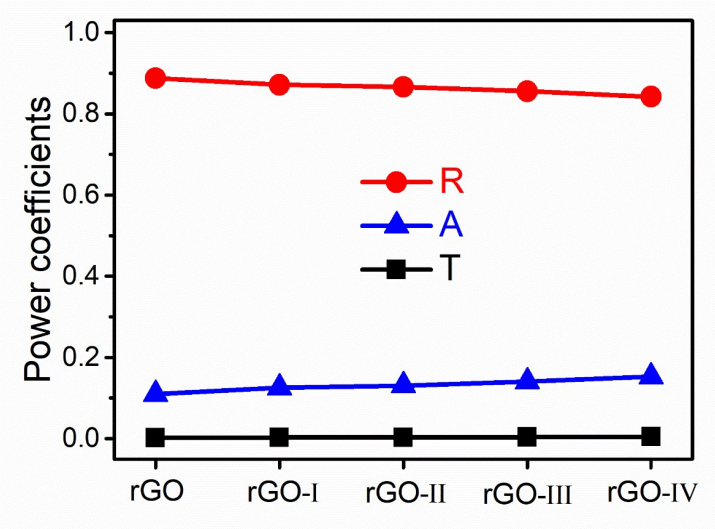

Fig. S5 Power coefficients of the rGO and rGO/CA films at 10.3 GHz.

6. SEM images and Ca-element mapping of the GO-Ca^{2+} and rGO-Ca^{2+} films

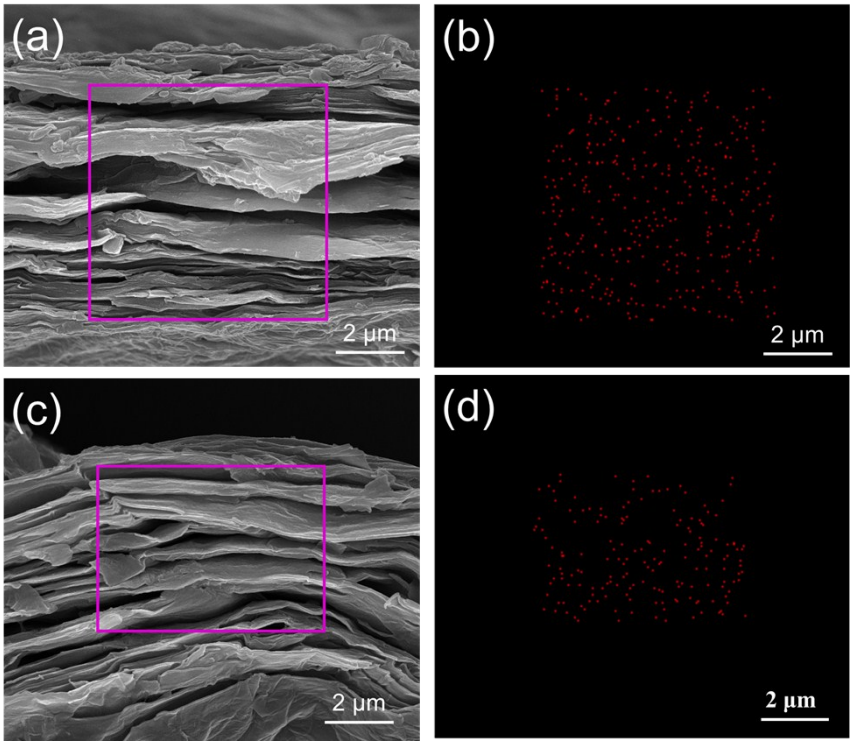

Fig. S6 SEM images of cross-sectional surface of (a) GO-Ca^{2+} film and the corresponding Ca-element mapping (b); SEM images of cross-sectional surface of (c) rGO-Ca^{2+} film and the corresponding Ca-element mapping (d).

7. Comparison of EMI SE of rGO/CA films in this work with the literature.

Table S1 EMI shielding performance for rGO/CA films compared with other carbon-based materials reported in the literature.

Materials	Thickness (mm)	EMI SE (dB)	Specific EMI SE (dB/mm)	Tensile strength and toughness (MPa@MJ/m^3)	Reference
rGO-I	**0.012**	**25.7**	**2142**	**118.0@4.6**	**This work**
rGO[a)]	0.0084	20.0	2381	~	2
rGO[a)]	0.015	20.2	1347	77.7@~	3
F-doped rGO[a)]	0.35	22.5	64		4
rGO/PVA[a)]	0.23	9.1	40	62.4@1.8	5
rGO-Fe_2O_3/PVA[a)]	0.36	20.3	56	55.2@2.4	5
rGO/CNF[a)]	0.023	26.2	1139	67.0@~	6
GNS[a)]	0.05	60.0	1200	22.0@~	7
GNS[a)]	0.1	19.0	190	~	8
GNS/CuPc[a)]	0.47	55.2	117	~	9
GNS/Fe_3O_4[a)]	0.2-0.25	22.0	88-110	~	10
GNS/EVA[a)]	0.35	25.0	71	~	11
GNS/AAP[a)]	0.03	36.0	1200	~	12
GNS/PDMS[a)]	1.0	20.0	20		13
GNS/PU[a)]	2.0	32.0	16		14
Pd-CNT-Cu	0.2	35.0	175	~	15
Co/Ni-CNT	1.0	12.0	12	~	16
CNT/PU[a)]	0.05	24.0	480		17
CNT/NR[a)]	0.05	21.4	428		18
CNT/cellulose	0.17	20.3	119		19
CNT/cellulose	0.15	35.0	233		20
CNT/PU[a)]	1.5	29.0	19		1
CNT/PU[a)]	2.0	17.0	9		21

CNT/PVDF[a)]	2.0	20.9	15	22
CNT/PANI[a)]	2.4	31.5	13	23
CF/cellulose	0.167	24.6	147	24
CF/ABS[a)]	1.1	26.1	24	25
CB/ABS[a)]	1.1	20.9	19	25
CB/EPDM[a)]	2.0	30.3	15	26
Graphite/PANI[a)]	2.0	33.6	17	27

[a)] rGO, PVA, CNF, GNS, CuPc, EVA, AAP, PDMS, PU, CNT, NR, PVDF, PANI, CF, CB, ABS and EPDM indicate reduced graphene oxide, polyvinyl alcohol, cellulose nanofiber, graphene, copper phthalocyanine, ethylene vinyl acetate, acrylic artists' paint, polydimethylsiloxane, polyurethane, carbon nanotube, natural rubber, polyvinylidene fluoride, polyaniline, carbon fiber, carbon black, acrylonitrile butadiene styrene-acrylonitrile butadiene styrene and ethylene propylene diene monomer, respectively.

References

[1] T. K. Gupta, B. P. Singh, S. R. Dhakate, V. N. Singh and R. B. Mathur, *J. Mater. Chem. A*, 2013, **1**, 9138-9149.

[2] B. Shen, W. T. Zhai and W. G. Zheng, *Adv. Funct. Mater.*, 2014, **24**, 4542-4548.

[3] P. Kumar, F. Shahzad, S. Yu, S. M. Hong, Y. H. Kim and C. M. Koo, *Carbon*, 2015, **94**, 494-500.

[4] F. Shahzad, S. A. Zaidi and C. M. Koo, *ACS Appl. Mater. Interfaces*, 2017, **9**, 24179-24189.

[5] B. Yuan, C. Bao, X. Qian, L. Song, Q. Tai, K. M. Liew and Y. Hu, *Carbon*, 2014, **75**, 178-189.

[6] W. Yang, Z. Zhao, K. Wu, R. Huang, T. Liu, H. Jiang, F. Chen and Q. Fu, *J. Mater. Chem. C*, 2017, **5**, 3748-3756.

[7] L. Zhang, N. T. Alvarez, M. Zhang, M. Haase, R. Malik, D. Mast and V. Shanov, *Carbon*, 2015, **82**, 353-359.

[8] W. L. Song, L. Z. Fan, M. S. Cao, M. M. Lu, C. Y. Wang, J. Wang, T. T. Chen, Y. Li, Z. L. Hou, J. Liu and Y. P. Sun, *J. Mater. Chem. C*, 2014, **2**, 5057-5064.

[9] Z. Wang, R. Wei and X. Liu, *ACS Appl. Mater. Interfaces*, 2017, **9**, 22408-22419.

[10] W. L. Song, X. T. Guan, L. Z. Fan, W. Q. Cao, C. Y. Wang, Q. L. Zhao and M.-S. Cao, *J. Mater. Chem. A*, 2015, **3**, 2097-2107.

[11] W. L. Song, M.-S. Cao, M. M. Lu, S. Bi, C. Y. Wang, J. Liu, J. Yuan and L. Z. Fan, *Carbon*, 2014, **66**, 67-76.

[12] J. E. Mates, I. S. Bayer, M. Salerno, P. J. Carroll, Z. Jiang, L. Liu and C. M. Megaridis, *Carbon*, 2015, **87**, 163-174.

[13] Z. Chen, C. Xu, C. Ma, W. Ren and H. M. Cheng, *Adv. Mater.*, 2013, **25**, 1296-1300.

[14] S. T. Hsiao, C. C. M. Ma, H. W. Tien, W. H. Liao, Y. S. Wang, S. M. Li and Y. C. Huang, *Carbon*, 2013, **60**, 57-66.

[15] A. Kumar, A. P. Singh, S. Kumari, A. Srivastava, S. Bathula, S. Dhawan, P. Dutta and A. Dhar, *J. Mater. Chem. A*, 2015, **3**, 13986-13993.

[16] B. Singh, D. Saket, A. Singh, S. Pati, T. Gupta, V. Singh, S. Dhakate, S. Dhawan, R. Kotnala and R. Mathur, *J. Mater. Chem. A*, 2015, **3**, 13203-13209.

[17] Z. Zeng, M. Chen, H. Jin, W. Li, X. Xue, L. Zhou, Y. Pei, H. Zhang and Z. Zhang, *Carbon*, 2016, **96**, 768-777.

[18] L. C. Jia, M. Z. Li, D. X. Yan, C. H. Cui, H. Y. Wu and Z. M. Li, *J. Mater. Chem.*

C, 2017, **5**, 8944-8951.

[19] T. W. Lee, S. E. Lee and Y. G. Jeong, *Compos. Sci. Technol.*, 2016, **131**, 77-87.

[20] L. Q. Zhang, B. Yang, J. Teng, J. Lei, D.-X. Yan, G. J. Zhong and Z. M. Li, *J. Mater. Chem. C*, 2017, **5**, 3130-3138.

[21] Z. Liu, G. Bai, Y. Huang, Y. Ma, F. Du, F. Li, T. Guo and Y. Chen, *Carbon*, 2007, **45**, 821-827.

[22] H. Wang, K. Zheng, X. Zhang, T. Du, C. Xiao, X. Ding, C. Bao, L. Chen and X. Tian, *Compos. Part A*, 2016, **90**, 606-613.

[23] T. K. Gupta, B. P. Singh, R. B. Mathur and S. R. Dhakate, *Nanoscale*, 2014, **6**, 842-851.

[24] S. Mondal, S. Ganguly, P. Das, P. Bhawal, T. K. Das, L. Nayak, D. Khastgir and N. C. Das, *Cellulose*, 2017, **24**, 5117-5131.

[25] M. H. Al-Saleh, W. H. Saadeh and U. Sundararaj, *Carbon*, 2013, **60**, 146-156.

[26] P. Ghosh and A. Chakrabarti, *Eur. Polym. J.*, 2000, **36**, 1043-1054.

[27] P. Sawai and S. Banerjee, *J. Appl. Polym. Sci.*, 2008, **109**, 2054-2063.